Supramolecular Chemistry
Publication details, including instructions for authors and subscription information:
http://www.informaworld.com/smpp/title~content=t713649759

Temperature-dependent spectral changes of self-aggregates of zinc chlorophylls esterified by different linear alcohols at the 17-propionate

Yoshitaka Saga[a]; Yuichi Nakai[a]; Hitoshi Tamiaki[b]
[a] Department of Chemistry, Faculty of Science and Engineering, Kinki University, Higashi-Osaka, Osaka, Japan [b] Department of Bioscience and Biotechnology, Faculty of Science and Engineering, Ritsumeikan University, Kusatsu, Shiga, Japan

To cite this Article Saga, Yoshitaka , Nakai, Yuichi and Tamiaki, Hitoshi(2009) 'Temperature-dependent spectral changes of self-aggregates of zinc chlorophylls esterified by different linear alcohols at the 17-propionate', Supramolecular Chemistry, 21: 8, 738 — 746
To link to this Article: DOI: 10.1080/10610270902853035
URL: http://dx.doi.org/10.1080/10610270902853035

Supramolecular Chemistry
Vol. 21, No. 8, December 2009, 738–746

Taylor & Francis
Taylor & Francis Group

Temperature-dependent spectral changes of self-aggregates of zinc chlorophylls esterified by different linear alcohols at the 17-propionate

Yoshitaka Saga[a]*, Yuichi Nakai[a] and Hitoshi Tamiaki[b]

[a]*Department of Chemistry, Faculty of Science and Engineering, Kinki University, Higashi-Osaka, Osaka 577-8502, Japan;* [b]*Department of Bioscience and Biotechnology, Faculty of Science and Engineering, Ritsumeikan University, Kusatsu, Shiga 525-8577, Japan*

(*Received 29 December 2008; final version received 24 February 2009*)

Systematically synthetic zinc 3-hydroxymethyl-13^1-oxo-chlorins esterified by different linear alcohols (methanol, 1-propanol, 1-hexanol, 1-dodecanol and 1-octadecanol) at the 17-propionate were self-assembled in the presence of cetyltrimethylammonium bromide in an aqueous solution. These zinc chlorins exhibited red-shifted Q_y absorption bands and circular dichroism (CD) signals in the corresponding Q_y region after incubation for 17 h, indicating that the zinc chlorins formed self-aggregates like those in natural chlorosomes of green photosynthetic bacteria. Visible absorption and CD spectra of self-aggregates of the zinc chlorins depended on the length of their esterifying alcohols. Zinc chlorins esterified by shorter alcohols gave larger changes in their visible absorption and CD spectra after incubation above 40°C, whereas zinc chlorins esterified by longer alcohols afforded smaller changes. These results indicate that hydrophobic interaction among esterifying chains of chlorin molecules as well as that between the esterifying chains and peripheral surfactants or lipids play an important role in the stability of chlorosomal self-aggregates.

Keywords: chlorin; chlorosome; green photosynthetic bacteria; hydrophobic interaction

Introduction

In the primary process of photosynthesis, light-harvesting complexes capture sunlight energy and transfer it to a reaction centre with high efficiency. In photosynthetic light-harvesting complexes, chlorophyll (Chl) and bacteriochlorophyll (BChl) molecules are well organised to form photofunctional apparatus. Most bacterial light-harvesting complexes consist of BChls and proteins, where the pigments are arranged in protein scaffolds. No protein participates in the organisation of BChls in major antenna complexes of green photosynthetic bacteria called chlorosomes (*1–5*). In chlorosomes, BChls *c*, *d* and *e* self-aggregate through pigment–pigment interaction, and the self-aggregates form rod-shaped or lamellar supramolecular structures in a lipid monolayer (*6–10*). The molecular structure of BChl *d* is shown in Figure 1(A). Essential parts of chlorosomal BChls such as BChl *d* for self-assembly are central magnesium, 3^1-hydroxy group and 13-keto group. In chlorosomal self-aggregates, central magnesium of one BChl molecule is coordinated by 3^1-hydroxy group of another BChl molecule and the hydroxy group is hydrogen-bonded to 13-keto group of a third BChl molecule (*1–5*). Hydrophobic interaction among long esterifying chains at the 17-propionate as well as $\pi-\pi$ stacking of chlorin macrocycles would also contribute to stabilisation of chlorosomal self-aggregates. However, there are fewer reports on the effects of esterifying chains at the 17-propionate of BChl molecules on chlorosomal self-assembly (*11–19*) than those concerning formation of both hydrogen and coordination bonds using three essential parts of BChl molecules.

BChl *c* molecules in the green sulphur bacterium *Chlorobium* (*Chl.*) *tepidum* are mainly esterified by a farnesol at the 17-propionate, whereas those in the thermophilic green filamentous bacterium *Chloroflexus* (*Cfl.*) *aurantiacus* have several linear (octadecanol and hexadecanol) and isoprenoid alcohols (phytol and geranylgeraniol) at this position (*1*, *11*). Miller and her co-workers (*12*, *13*) succeeded in changing *in vivo* composition of the esterifying alcohols of BChl *c* in both *Chl. tepidum* and *Cfl. aurantiacus* by cultivating them in liquid cultures containing exogenous alcohols. However, little effect on spectral properties of natural chlorosomes was observed: the only detectable change was a slight blue-shift (6 nm) of the Q_y band in *Chl. tepidum* cells, in which 43% BChl *c* was esterified by dodecanol.

Tamiaki *et al*. (*14*) have reported *in vitro* self-aggregates of synthetic zinc 3-hydroxymethyl-13^1-oxo-chlorins possessing branched alkyl chains and semi-synthetic 3^1*R*-8-ethyl-12-ethyl-BChl *c* esterified by linear alcohols (*17*). Branched alkyl chains at the 17-propionate of the synthetic zinc chlorins little affected visible absorption spectra of the self-aggregates but changed their circular dichroism (CD) spectra (*14*). Linear alkyl

*Corresponding author. Email: saga@chem.kindai.ac.jp

ISSN 1061-0278 print/ISSN 1029-0478 online

DOI: 10.1080/10610270902853035
http://www.informaworld.com

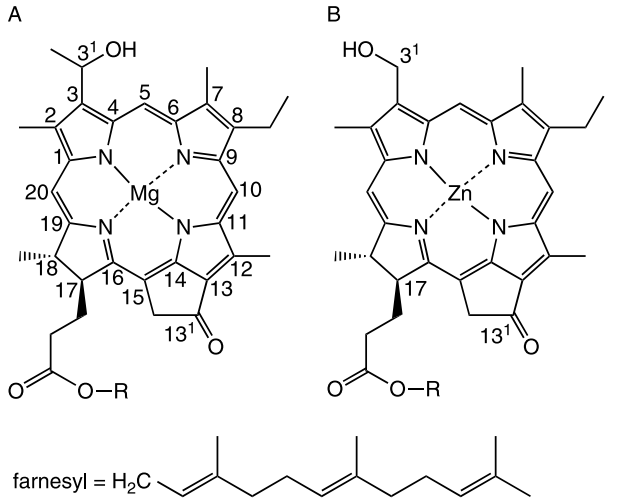

Figure 1. Molecular structures of 8-ethyl-12-methyl-BChl *d* (A) and zinc chlorins **1**–**5** used in the present study (B). BChl *d*: R = farnesyl (major), **1**: R = CH_3, **2**: R = $(CH_2)_2CH_3$, **3**: R = $(CH_2)_5CH_3$, **4**: R = $(CH_2)_{11}CH_3$ and **5**: R = $(CH_2)_{17}CH_3$.

chains of the semi-synthetic magnesium chlorins also little changed the visible absorption spectra and sizes of their self-aggregates in Triton X-100 micelles, although they would affect deaggregation behaviour by additive 1-hexanol (*17*). Recently, Zupcanova *et al*. (*18*) also reported self-assembly of BChl *c* esterified by several alcohols in aqueous buffer and nonpolar alkanes, where the length of esterifying alcohols affected Q_y absorption bands in their visible absorption spectra. Both *in vivo* and *in vitro* studies suggested that esterifying alcohols at the 17-propionate had slight influence on BChl organisation in chlorosomal self-aggregates. However, effects of the length of esterifying chains of chlorosome-type chlorins on the stability of self-aggregates have not been thoroughly examined yet.

We report herein the temperature-dependent spectral changes of self-aggregates of five systematically synthetic zinc 3-hydroxymethyl-13^1-oxo-chlorins **1**–**5** (see Figure 1(B)), which were esterified by methanol, 1-propanol, 1-hexanol, 1-dodecanol and 1-octadecanol, respectively, at the 17-propionate, in the presence of cetyltrimethylammonium bromide (CTAB) in aqueous phase to unravel the role of esterifying alcohols in the stability of chlorosomal self-assembly.

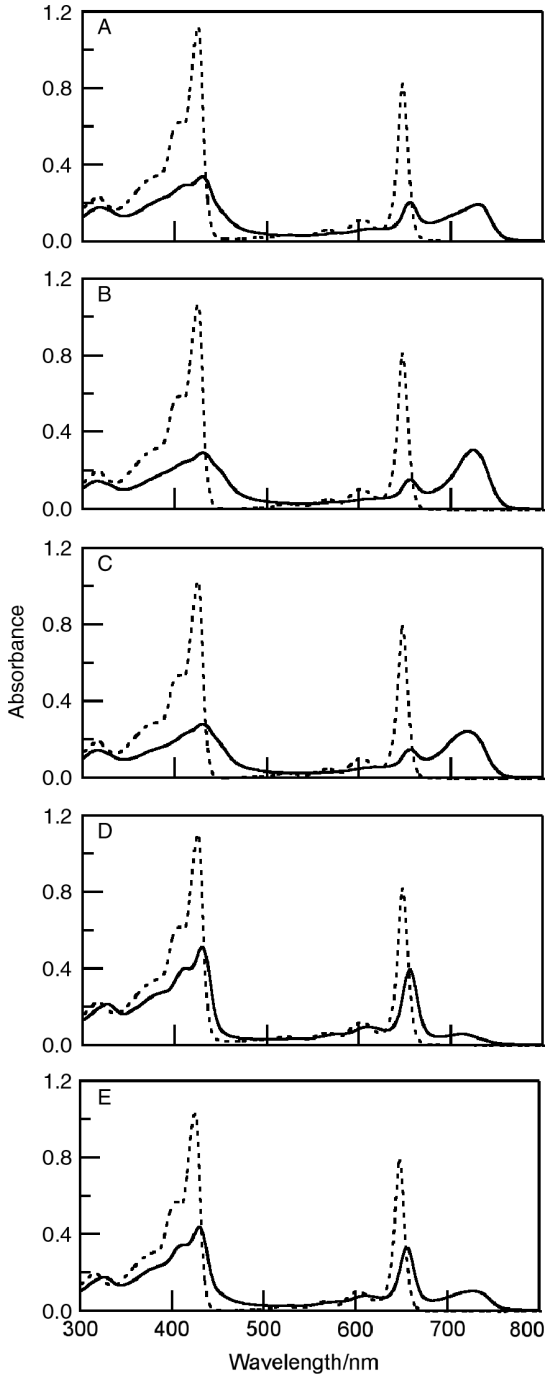

Figure 2. Visible absorption spectra of self-aggregates in the presence of CTAB in an aqueous solution just after preparation (solid curve) and monomers in THF (broken curve) of zinc chlorins **1** (A), **2** (B), **3** (C), **4** (D) and **5** (E).

Results and discussion

Figure 2 depicts the visible absorption spectra of self-aggregates of zinc chlorins **1**–**5** in the presence of CTAB in an aqueous solution just after preparation and their monomeric forms in THF. Zinc chlorins **1**–**5** exhibited the same visible absorption spectra in THF, whereas Soret and Q_y absorption bands were as positioned at 424 and 647 nm, respectively, indicating that substitution at the 17-propionate did not disturb the electronic structure of the chlorin π-system. In an aqueous solution, zinc chlorins **1**–**5** had Q_y absorption bands in the wavelength region between 715 and 730 nm, which were red-shifted by *ca.*

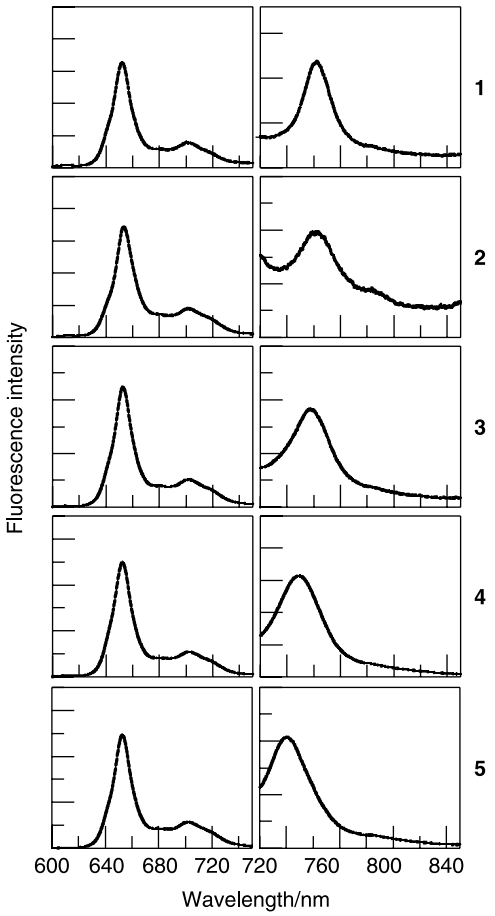

Figure 3. Fluorescence spectra of monomers in THF (left column) and self-aggregates in the presence of CTAB in an aqueous solution just after preparation (right column) of zinc chlorins **1**–**5**. Excitation wavelength, 427 and 450 nm for monomers and self-aggregates, respectively.

70–85 nm compared with those of the monomeric forms. Soret absorption bands of zinc chlorins **1**–**5** with CTAB in an aqueous solution were also shifted to a longer wavelength than those of the monomers. These visible absorption spectral changes were characteristic of BChl self-assembly in natural chlorosomes. The Q_y absorption maxima of self-aggregates of **1**–**5** were similar to each other, although the relative ratio of Q_y absorbance of self-aggregates around 715–730 nm to that of residual monomers at 656 nm was different.

Fluorescence spectra of monomers in THF and self-aggregates of zinc chlorins **1**–**5** in the presence of CTAB in an aqueous solution just after preparation are shown in Figure 3. Monomeric forms of **1**–**5** exhibited the same fluorescence spectra in THF, where emission bands were positioned at 653 nm. In contrast, self-aggregates of zinc chlorins **1**–**5** had fluorescence emission bands around 725–740 nm, which were shifted to a longer wavelength compared with those of the monomers. These fluorescence bands of self-aggregates of **1**–**5** were similar to each other. Spectral properties by visible absorption, CD and fluorescence spectroscopy suggest that zinc chlorins **1**–**5** self-assembled like chlorosomes.

Self-aggregates of zinc chlorins **1**–**5** in an aqueous solution were incubated at 40, 50 and 60°C as well as room temperature for 17 h, and visible absorption and CD spectra of self-aggregates were measured. Figure 4 depicts visible absorption spectra of self-aggregates of **1**–**5** after incubation. By incubation above 40°C, zinc chlorin **1** exhibited a slightly red-shifted Q_y peak and increase in Q_y absorbance of self-aggregates accompanying decrease in monomeric Q_y absorbance. Bandwidths, full widths at half maxima (FWHMs), of Q_y absorption bands of self-aggregates of **1** after incubation at 40, 50 and 60°C were 919, 743 and 856 cm^{-1}, respectively, which were similar to each other. Elongation of esterified chains at the 17-propionate of zinc chlorins displayed different behaviour by incubation. In the cases of zinc chlorins **2** and **3**, incubation at 40°C resulted in a slight red-shift of the Q_y peak position of self-aggregates compared to the case by incubation at room temperature, but Q_y absorbance of self-aggregates little increased. In contrast, incubation at 50 and 60°C induced further red-shift and increase of absorbance in Q_y absorption bands. In addition, Q_y absorption bands of self-aggregates were sharpened by incubation at 50 and 60°C. FWHMs of Q_y bands of self-aggregates of **2** after incubation at 50 and 60°C were 495 and 530 cm^{-1}, respectively, and those of **3** after incubation at 50 and 60°C were 626 and 588 cm^{-1}, respectively. These values were smaller than those after incubation at 40°C (894 and 854 cm^{-1} for **2** and **3**, respectively). These indicate that incubation at 50 and 60°C changed absorption spectra of self-aggregates of **2** and **3** more largely than those at 40°C. Q_y peak positions of self-aggregates of zinc chlorins **4** and **5** were slightly shifted to a shorter wavelength by incubation above 40°C than that by incubation at room temperature. Q_y bandwidths of self-aggregates of **4** and **5** scarcely depended on incubation temperature. Zinc chlorin **5** had a large monomeric Q_y band at 656 nm by incubation at room temperature, and increased Q_y absorbance of self-aggregates by incubation above 40°C.

Since CD spectroscopy is more sensitive to supramolecular structures of chlorosomal self-aggregates than visible absorption spectroscopy, CD spectra are expected to provide more detailed information on structural changes of self-aggregates of zinc chlorins **1**–**5** by incubation. Figure 5 depicts CD spectra of self-aggregates of **1**–**5** after incubation. Zinc chlorins **1**–**3** exhibited S-shaped CD signals in both Soret and Q_y regions, whereas zinc chlorin **4** exhibited reverse S-shaped CD signals after incubation. The reverse of CD shapes of self-aggregates of zinc chlorins possessing longer esterifying chains at the 17-propionate was consistent with the previous report (*14*).

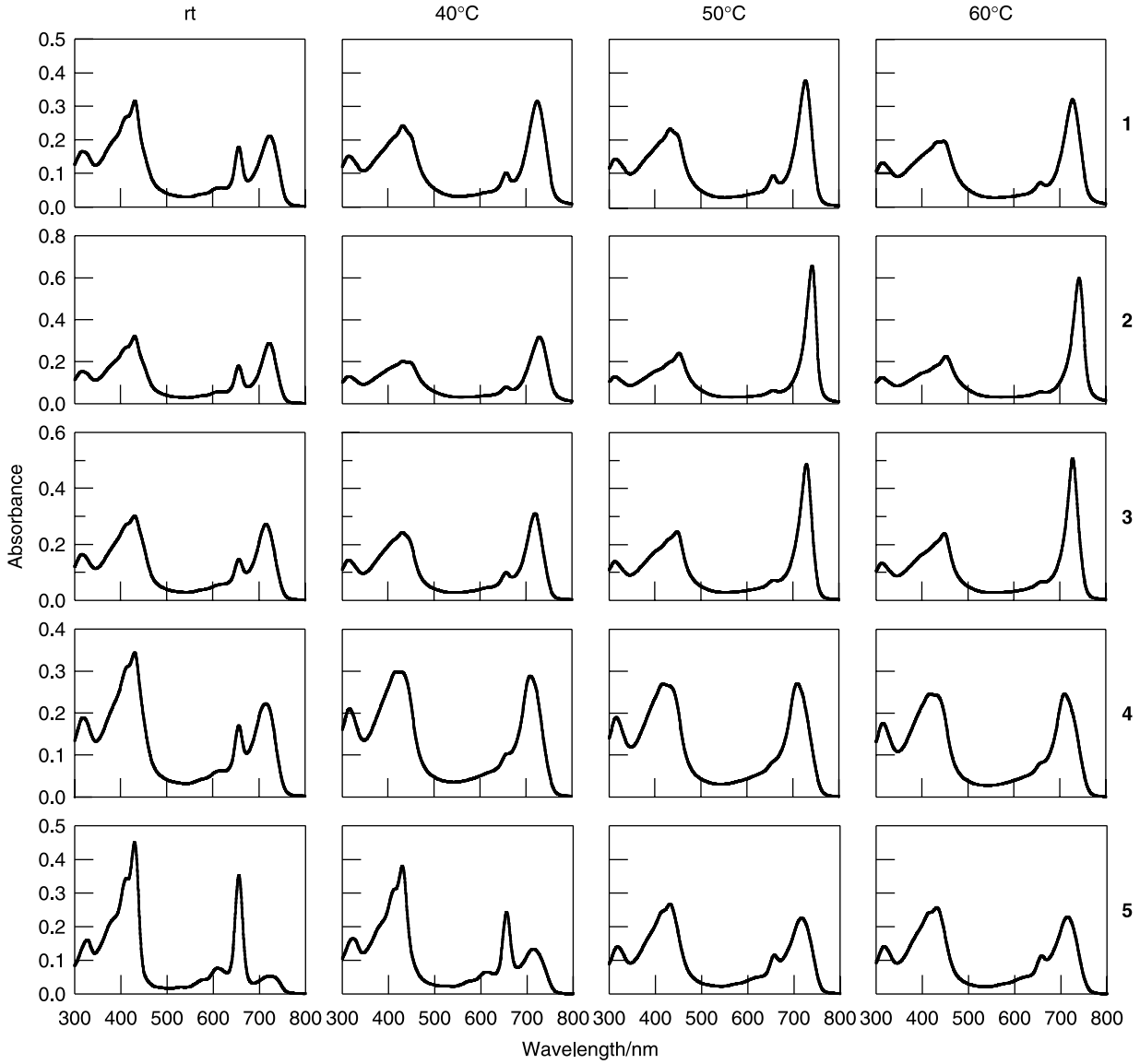

Figure 4. Visible absorption spectra of self-aggregates of zinc chlorins **1**–**5** in the presence of CTAB in an aqueous solution after incubation at room temperature, 40, 50 and 60°C for 17 h.

CD signals of self-aggregates of zinc chlorin **5** was very small. The intensity of CD signals in the Q_y regions of self-aggregates of **1** increased six to seven times (comparison of positive signals) and the position was slightly red-shifted after incubation above 40°C compared with that after incubation at room temperature. The red-shift of CD signals corresponded to that in visible absorption spectra. Self-aggregates of **2** after incubation at 40, 50 and 60°C exhibited CD signals in the Q_y region, which was 9-, 13- and 13-times, respectively, larger than that after incubation at room temperature (comparison of positive signals). CD spectra of self-aggregates of zinc chlorin **3** after incubation were different from those of zinc chlorins **1** and **2**, and significantly depended on incubation temperature. Namely, CD signal of **3** in the Q_y region after incubation at 40°C was only two times larger than that after incubation at room temperature, while CD signals of self-aggregates after incubation at 50 and 60°C increased six and nine times, respectively (comparison of positive signals). Such a significant increase in CD intensity of self-aggregates of **1**–**3** would originate from structural changes of self-aggregates rather than only conversion from the monomeric form to aggregates, since CD intensity of self-aggregates of **1** and **2** above 40°C and **3** above 50°C, which were normalised by Q_y absorbance, was four to six times larger. Increase in CD intensity by incubation above 40°C was small and hardly observed in self-aggregates of zinc chlorins **4** and **5**, respectively. These small and barely

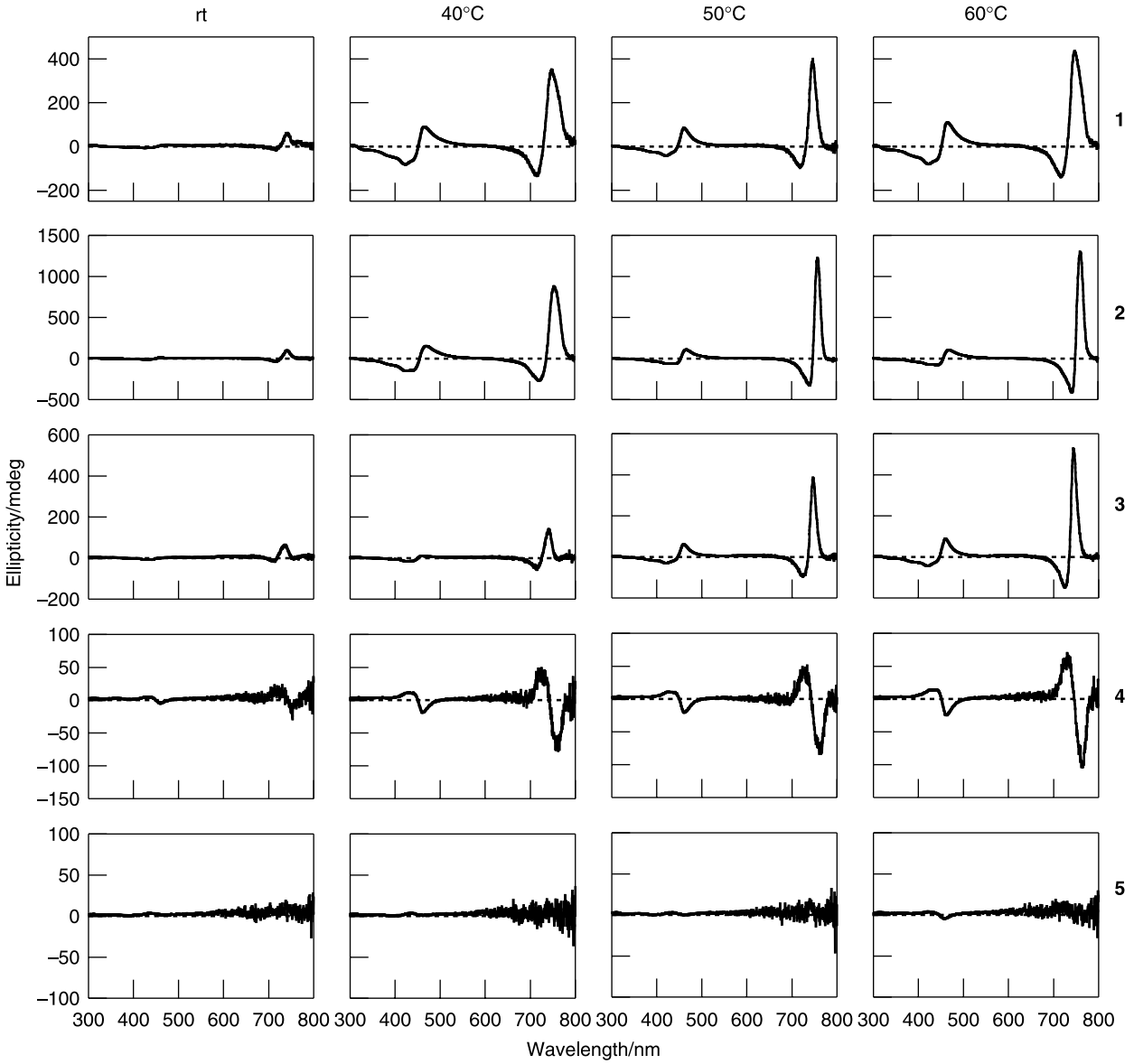

Figure 5. CD spectra of self-aggregates of zinc chlorins **1**–**5** in the presence of CTAB in an aqueous solution after incubation at room temperature, 40, 50 and 60°C for 17 h.

observable changes in CD spectra of **4** and **5** would be ascribable to tolerance to structural changes of self-aggregates by strong hydrophobic interaction among long esterifying chains as well as that between the esterifying chains and hexadecyl groups of CTAB. Both visible absorption and CD spectra of self-aggregates of zinc chlorins **1**–**5** after incubation at different temperature indicate that elongation of esterifying chains at the 17-propionate stabilises supramolecular structures of self-aggregates of chlorins by hydrophobic interaction.

Temporal changes of Q_y maximum absorbance and maximum intensity of the positive CD signals in the Q_y region of self-aggregates of zinc chlorins **1**–**5** by incubation are shown in Figures 6 and 7, respectively. Q_y absorbance of self-aggregates of **1**–**5** was little changed by incubation at room temperature. In contrast, Q_y absorbance of self-aggregates of **2**–**5** was increased within 5 h at 50 and 60°C. Incubation at 40°C also increased Q_y absorbance of self-aggregates of **3** and **4** within 5 h.

Positive CD signals in the Q_y region of self-aggregates of zinc chlorins **1**–**3** increased within 5 h at 60°C. By incubation at 50°C, CD signals of self-aggregates of **1** and **3** became almost constant for 5 h, but those of **2** gradually increased after 5 h. Incubation at 40°C increased CD signals of **1**–**3** more slowly than incubation at 50 and 60°C. These suggest that supramolecular structures of

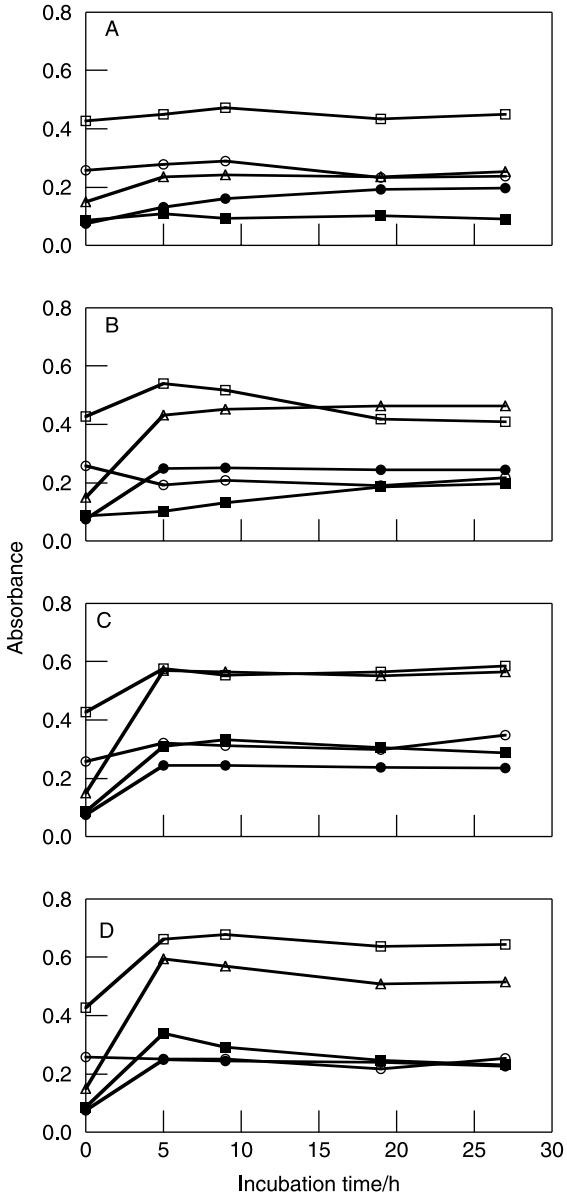

Figure 6. Temporal changes of Q_y maximum absorbance of self-aggregates of zinc chlorins **1** (open circle), **2** (open square), **3** (open triangle), **4** (closed circle) and **5** (closed square) in the presence of CTAB in an aqueous solution by incubation at room temperature (A), 40 (B), 50 (C) and 60°C (D).

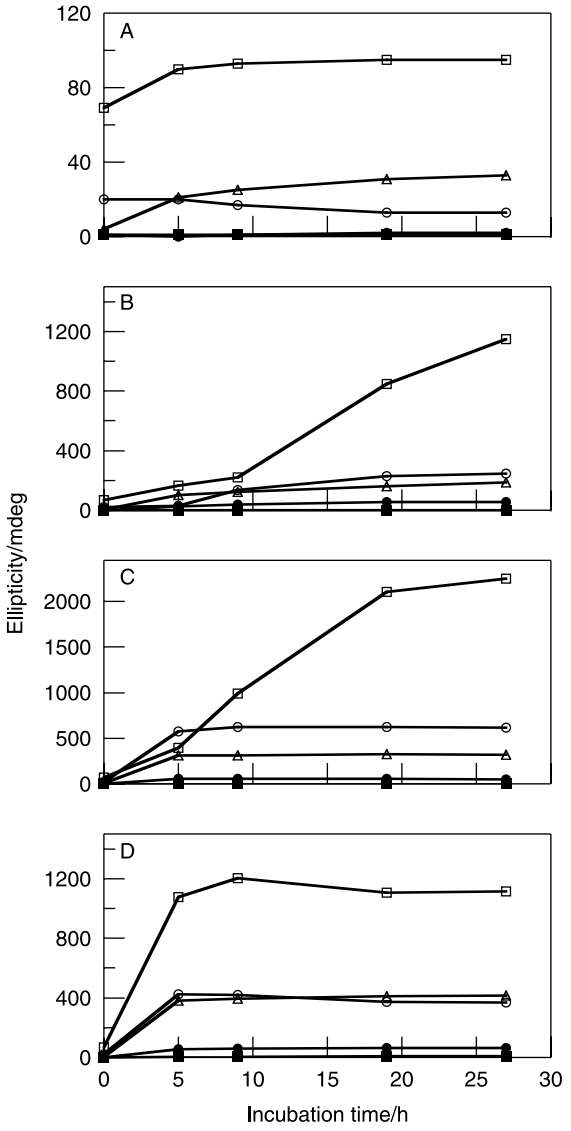

Figure 7. Temporal changes of maximum intensity of the positive CD signals in the Q_y region of self-aggregates of zinc chlorins **1** (open circle), **2** (open square), **3** (open triangle), **4** (closed circle) and **5** (closed square) in the presence of CTAB in an aqueous solution by incubation at room temperature (A), 40 (B), 50 (C) and 60°C (D).

self-aggregates of **1**–**3** changed rapidly at higher temperature. In contrast, self-aggregates of **4** and **5** would be more tolerant to structural changes than those of **1**–**3** by strong hydrophobic interaction among long hydrocarbon chains.

Proposed structural changes of self-aggregates of zinc chlorins esterified by linear alcohols by incubation are summarised in Figure 8. Zinc chlorins assembled by their hydrophobic interaction as a main driving force just after preparation in aqueous media, and the organisation of the resulting chlorosomal aggregates might be somewhat moderate. Self-aggregates of zinc chlorins esterified by shorter alcohols would convert to a highly organised forms, which have large CD signals, by thermal energy, whereas those of zinc chlorins esterified by longer alcohols could hardly change due to strong hydrophobic interactions of esterifying chains.

The effect of hydrophobic interaction of esterifying alcohols of chlorosomal chlorins on the stability of their self-aggregates would have biological meaning in chlorosomal structures and functions of green

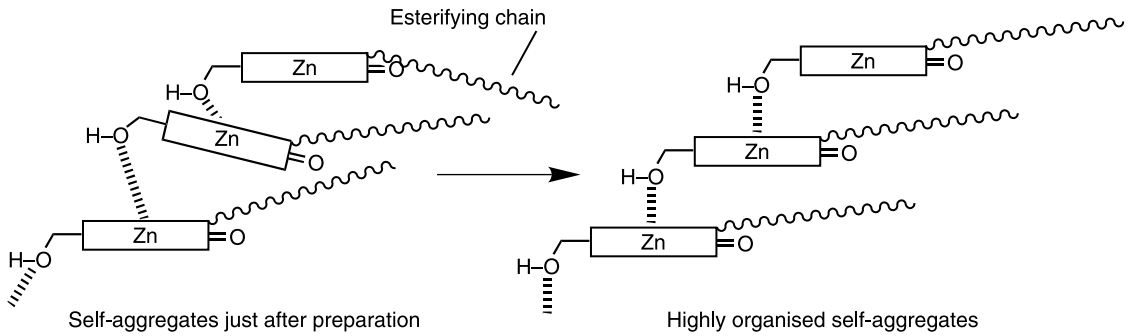

Figure 8. Proposed structural changes of self-aggregates of zinc chlorins esterified by linear alcohols by incubation.

photosynthetic bacteria. A green sulphur bacterium *Chl. tepidum*, whose optimal growth temperature is 47°C (*20*), possesses BChl *c* esterified by farnesol (C_{15}). In contrast, a green filamentous bacterium *Cfl. aurantiacus*, which grows at higher temperature 55°C (*21*), has BChl *c* esterified by longer alcohols such as octadecanol (C_{18}) and phytol (C_{20}) than that of *Chl. tepidum*. Carbon numbers of esterifying chains in zinc chlorins **4** and **5** (C_{12} and C_{18}, respectively) correspond to those of an alkyl chain except branched methyl groups of farnesol (C_{12}) and octadecanol (C_{18}). Therefore, the small and barely observable spectral changes of self-aggregates of **4** and **5**, respectively, suggest that BChl *c* in thermophilic green photosynthetic bacteria is esterified by sufficiently long alcohols which can maintain supramolecular structures of chlorosomal self-aggregates by their hydrophobic interaction. Esterifying alcohols of chlorosomal BChls might be selected through the evolution process of green photosynthetic bacteria to stabilise supramolecular structures of BChl self-aggregates and suppress the loss of captured light-energy by fluctuation in the aggregates even at a high growth temperature.

Experimental

Apparatus and materials

Visible absorption and CD spectra were measured with a Shimadzu UV-2450 spectrophotometer and a JASCO J-720 spectropolarimeter, respectively. Fluorescence spectra were measured with a Hitachi F-4500 spectrophotometer. The ^{1}H NMR spectra were measured with a JEOL JNM-AL400 NMR spectrometer; chemical shifts are expressed (in ppm) relative to $CHCl_3$ (7.26) as an internal reference. Mass spectra were measured with a Shimadzu KOMPACT MALDI 4 spectrometer. High performance liquid chromatography (HPLC) was performed with a Shimadzu LC-20AT pump and an SPD-20AV detector. Pyropheophorbide *d* was prepared from Chl *a*, which was extracted from *Spirulina geitleri* according to the previous report (*22*).

Preparation of self-aggregates

Self-aggregates of synthetic zinc chlorins were prepared in essentially the same procedure as the previous reports (*23*, *24*). Synthetic zinc chlorins were dissolved in THF (30 μl) and mixed with a methanol solution of CTAB (10 μl), followed by dispersion into 3960 μl of distilled water. Final concentrations of zinc chlorins and CTAB in the aqueous solution were 7.5 μM and 0.0425% (w/v), respectively.

Esterification of pyropheophorbide a *with a saturated alcohol*

Pyropheophorbide *d* was dissolved in distilled CH_2Cl_2, and five equivalents of a saturated alcohol, 1-ethyl-3-(3-dimethylaminopropyl)carbodiimide hydrochloride (EDC·HCl), 4-(*N*,*N*-dimethylamino)pyridine, and one drop of triethylamine were added to the solution. The reaction mixture was stirred overnight at room temperature under nitrogen in the dark. Then, 2% HCl was added to the reaction mixture, and extracted with CH_2Cl_2, washed with aqueous 4% $NaHCO_3$, distilled water and dried over Na_2SO_4. After evaporation, the residue was purified by flash column chromatography (FCC) and recrystallisation to give pyropheophorbide *d* alkyl ester.

Reduction of 3-formyl to 3-hydroxymethyl group

tert-Butylamine borane complex was added to a CH_2Cl_2 solution of the above 3-formyl chlorin, and stirred at room temperature under nitrogen in the dark. After disappearance of 3-formyl chlorin using visible absorption spectral analyses, 2% HCl was added to the reaction mixture. The mixture was then extracted with CH_2Cl_2, washed with aqueous 4% $NaHCO_3$, distilled water and dried over Na_2SO_4. After evaporation, the residue was purified by FCC and recrystallisation to give 3-hydroxymethyl chlorin.

Zinc insertion

A methanol solution saturated with $Zn(CH_3COO)_2{\cdot}2H_2O$ was added to a CH_2Cl_2 solution of the above metal-free

3-hydroxymethyl chlorin and stirred at room temperature under nitrogen in the dark. After disappearance of metal-free chlorin using visible absorption spectral analyses, aqueous 4% $NaHCO_3$ was added to the reaction mixture, and stirred for 15 min. After filtration, the mixture was extracted with CH_2Cl_2, washed with distilled water and dried over Na_2SO_4. After evaporation, the residue was purified by recrystallisation to give zinc-inserted chlorin. The zinc complexes were purified by reverse-phase HPLC before preparation of self-aggregates.

Spectral data

3-Devinyl-3-hydroxymethyl-pyropheophorbide a *methyl ester*

UV–vis (CH_2Cl_2) λ_{max}(nm): 662 (relative intensity, 0.47), 606 (0.08), 536 (0.09), 505 (0.10), 410 (1.00). ^{1}H NMR ($CDCl_3$): δ (ppm) 9.47, 9.40, 8.62 (each 1H, s, 5-, 10-, 20-H), 5.75 (2H, s, 3-CH_2), 5.23, 5.08 (each 1H, d, $J = 20$ Hz, 13^2-H_2), 4.53–4.49 (1H, m, 18-H), 4.31–4.27 (1H, m, 17-H), 3.72–3.64 (5H, m, 8-CH_2 + 17^2-$COOCH_3$), 3.59, 3.35, 3.21 (each 3H, s, 2-, 7-, 12-CH_3), 2.71–2.65, 2.63–2.56, 2.33–2.28 (1H + 1H + 2H, m, 17-CH_2CH_2), 1.82 (3H, d, $J = 7$ Hz, 18-CH_3), 1.66 (3H, t, $J = 8$ Hz, 8^1-CH_3), −0.06, −1.98 (each 1H, s, NH). MS (MALDI): found (*m*/*z*) 553; calcd for $C_{33}H_{37}N_4O_4$ [MH^+], 553.

3-Devinyl-3-hydroxymethyl-pyropheophorbide a *propyl ester*

UV–vis (CH_2Cl_2) λ_{max} (nm): 662 (relative intensity, 0.45), 606 (0.08), 536 (0.09), 505 (0.09), 410 (1.00). ^{1}H NMR ($CDCl_3$): δ (ppm) 9.41, 9.38, 8.62 (each 1H, s, 5-, 10-, 20-H), 5.73 (2H, s, 3-CH_2), 5.21, 5.07 (each 1H, d, $J = 20$ Hz, 13^2-H_2), 4.53–4.49 (1H, m, 18-H), 4.31–4.26 (1H, m, 17-H), 4.05–3.95 (2H, m, 17^2-$COOCH_2$), 3.62 (2H, q, $J = 8$ Hz, 8-CH_2), 3.55, 3.34, 3.18 (each 3H, s, 2-, 7-, 12-CH_3), 2.70–2.63, 2.61–2.55, 2.33–2.28 (1H + 1H + 2H, m, 17-CH_2CH_2), 1.82 (3H, d, $J = 7$ Hz, 18-CH_3), 1.63 (3H, t, $J = 8$ Hz, 8^1-CH_3), 1.27–1.25 (2H, m, 17^2-$COOCCH_2$), 0.85 (3H, t, $J = 7$ Hz, 17^2-$COOC_2CH_3$), −0.12, −2.02 (each 1H, s, NH). MS (MALDI): found (*m*/*z*) 581; calcd for $C_{35}H_{41}N_4O_4$ [MH^+], 581.

3-Devinyl-3-hydroxymethyl-pyropheophorbide a *hexyl ester*

UV–vis (CH_2Cl_2) λ_{max} (nm): 662 (relative intensity, 0.48), 606 (0.08), 536 (0.09), 505 (0.09), 410 (1.00). ^{1}H NMR ($CDCl_3$): δ (ppm) 9.36, 9.35, 8.54 (each 1H, s, 5-, 10-, 20-H), 5.80 (2H, s, 3-CH_2), 5.16, 5.02 (each 1H, d, $J = 20$ Hz, 13^2-H_2), 4.45 (1H, dq, $J = 2$, 8 Hz, 18-H), 4.22 (1H, dt, $J = 9$, 2 Hz, 17-H), 4.05–3.96 (2H, m, 17^2-$COOCH_2$), 3.62 (2H, q, $J = 8$ Hz, 8-CH_2), 3.55, 3.37, 3.21 (each 3H, s, 2-, 7-, 12-CH_3), 2.67–2.59, 2.57–2.49, 2.30–2.20 (1H + 1H + 2H, m, 17-CH_2CH_2), 1.78 (3H, d, $J = 7$ Hz, 18-CH_3), 1.65 (3H, t, $J = 8$ Hz, 8^1-CH_3), 1.26–1.19 (8H, m, 17^2-$COOCC_4H_8$), 0.83 (3H, t, $J = 7$ Hz, 17^2-$COOC_5CH_3$), 0.01, −1.96 (each 1H, s, NH). MS (MALDI): found (*m*/*z*) 623; calcd for $C_{38}H_{47}N_4O_4$ [MH^+], 623.

3-Devinyl-3-hydroxymethyl-pyropheophorbide a *dodecyl ester*

UV–vis (CH_2Cl_2) λ_{max} (nm): 662 (relative intensity, 0.47), 606 (0.08), 536 (0.10), 505 (0.10), 410 (1.00). ^{1}H NMR ($CDCl_3$): δ (ppm) 9.38, 9.37, 8.56 (each 1H, s, 5-, 10-, 20-H), 5.81 (2H, s, 3-CH_2), 5.18, 5.04 (each 1H, d, $J = 20$ Hz, 13^2-H_2), 4.46 (1H, dq, $J = 2$, 8 Hz, 18-H), 4.24 (1H, dt, $J = 9$, 2 Hz, 17-H), 4.05–3.96 (2H, m, 17^2-$COOCH_2$), 3.63 (2H, q, $J = 8$ Hz, 8-CH_2), 3.56, 3.38, 3.21 (each 3H, s, 2-, 7-, 12-CH_3), 2.68–2.60, 2.58–2.49, 2.30–2.19 (1H + 1H + 2H, m, 17-CH_2CH_2), 1.79 (3H, d, $J = 7$ Hz, 18-CH_3), 1.65 (3H, t, $J = 8$ Hz, 8^1-CH_3), 1.22–1.18 (20H, m, 17^2-$COOCC_{10}H_{20}$), 0.85 (3H, t, $J = 7$ Hz, 17^2-$COOC_{11}CH_3$), 0.02, −1.95 (each 1H, s, NH). MS (MALDI): found (*m*/*z*) 707; calcd for $C_{44}H_{59}N_4O_4$ [MH^+], 707.

3-Devinyl-3-hydroxymethyl-pyropheophorbide a *octadecyl ester*

UV–vis (CH_2Cl_2) λ_{max} (nm): 662 (relative intensity, 0.45), 606 (0.08), 536 (0.09), 505 (0.09), 410 (1.00). ^{1}H NMR ($CDCl_3$): δ (ppm) 9.48, 9.45, 8.60 (each 1H, s, 5-, 10-, 20-H), 5.86 (2H, s, 3-CH_2), 5.24, 5.08 (each 1H, d, $J = 20$ Hz, 13^2-H_2), 4.50 (1H, dq, $J = 2$, 7 Hz, 18-H), 4.31–4.27 (1H, m, 17-H), 4.05–3.93 (2H, m, 17^2-$COOCH_2$), 3.68 (2H, q, $J = 8$ Hz, 8-CH_2), 3.62, 3.40, 3.24 (each 3H, s, 2-, 7-, 12-CH_3), 2.72–2.64, 2.59–2.51, 2.32–2.24 (1H + 1H + 2H, m, 17-CH_2CH_2), 1.81 (3H, d, $J = 7$ Hz, 18-CH_3), 1.67 (3H, t, $J = 8$ Hz, 8^1-CH_3), 1.23–1.18 (32H, m, 17^2-$COOCC_{16}H_{32}$), 0.87 (3H, t, $J = 7$ Hz, 17^2-$COOC_{17}CH_3$), 0.07, −1.89 (each 1H, s, NH). MS (MALDI): found (*m*/*z*) 792; calcd for $C_{50}H_{71}N_4O_4$ [MH^+], 792.

Zinc 3-devinyl-3-hydroxymethyl-pyropheophorbide a *methyl ester* (***1***)

UV–vis (THF) λ_{max} (nm): 647 (relative intensity, 0.73), 602 (0.10), 565 (0.06), 522 (0.04), 424 (1.00), 404 (0.56). MS (MALDI): found (*m*/*z*) 615; calcd for $C_{33}H_{35}N_4O_4Zn$ [MH^+], 615.

Zinc 3-devinyl-3-hydroxymethyl-pyropheophorbide a *propyl ester* (***2***)

UV–vis (THF) λ_{max} (nm): 647 (relative intensity, 0.76), 602 (0.10), 565 (0.05), 522 (0.03), 424 (1.00), 404 (0.55).

MS (MALDI): found (*m*/*z*) 643; calcd for $C_{35}H_{39}N_4O_4Zn$ [MH^+], 643.

Zinc 3-devinyl-3-hydroxymethyl-pyropheophorbide a *hexyl ester (**3**)*

UV–vis (THF) λ_{max} (nm): 647 (relative intensity, 0.77), 602 (0.10), 565 (0.05), 522 (0.03), 424 (1.00), 404 (0.52). MS (MALDI): found (*m*/*z*) 685; calcd for $C_{38}H_{45}N_4O_4Zn$ [MH^+], 685.

Zinc 3-devinyl-3-hydroxymethyl-pyropheophorbide a *dodecyl ester (**4**)*

UV–vis (THF) λ_{max} (nm): 647 (relative intensity, 0.74), 602 (0.11), 565 (0.06), 522 (0.04), 424 (1.00), 404 (0.56). MS (MALDI): found (*m*/*z*) 769; calcd for $C_{44}H_{57}N_4O_4Zn$ [MH^+], 769. See also Ref. (*19*).

Zinc 3-devinyl-3-hydroxymethyl-pyropheophorbide a *octadecyl ester (**5**)*

UV–vis (THF) λ_{max} (nm): 647 (relative intensity, 0.76), 602 (0.10), 565 (0.05), 522 (0.03), 424 (1.00), 404 (0.55). MS (MALDI): found (*m*/*z*) 853; calcd for $C_{50}H_{69}N_4O_4Zn$ [MH^+], 853.

Acknowledgements

This work was partially supported by Grants-in Aid for Young Scientists (B) (Nos 18750158/20750143) from MEXT, and for Scientific Research (B) (No. 19350080) from the Japan Society for the Promotion Science, and by the Kansai Research Foundation for Technology Promotion, the Mazda Foundation and Sekisui Integrated Research, Inc.

References

(1) Olson, J.M. *Photochem. Photobiol.* **1998**, *67*, 61–75.
(2) van Rossum, B.-J.; Steensgaard, D.B.; Mulder, F.M.; Boender, G.J.; Schaffner, K.; Holzwarth, A.R.; de Groot, H.J.M. *Biochemistry* **2001**, *40*, 1587–1595.
(3) Balaban, T.S.; Tamiaki, H.; Holzwarth, A.R. *Top. Curr. Chem.* **2005**, *258*, 1–38.
(4) Miyatake, T.; Tamiaki, H. *J. Photochem. Photobiol. C: Photochem. Rev.* **2005**, *6*, 89–107.
(5) Egawa, A.; Fujiwara, T.; Mizoguchi, T.; Kakitani, Y.; Koyama, Y.; Akutsu, H. *Proc. Natl Acad. Sci. USA* **2007**, *104*, 790–795.
(6) Staehelin, L.A.; Golecki, J.R.; Fuller, R.C.; Drews, G. *Arch. Microbiol.* **1978**, *119*, 269–277.
(7) Hohmann-Marriott, M.F.; Blankenship, R.E.; Roberson, R.W. *Photosynth. Res.* **2005**, *86*, 145–154.
(8) Saga, Y.; Tamiaki, H. *J. Biosci. Bioeng.* **2006**, *102*, 118–123.
(9) Psencík, J.; Ikonen, T.P.; Laurinmäki, P.; Merckel, M.C.; Butcher, S.J.; Serimaa, R.E.; Tuma, R. *Biophys. J.* **2004**, *87*, 1165–1172.
(10) Oostergetel, G.T.; Reus, M.; Chew, A.G.M.; Bryant, D.A.; Boekema, E.J.; Holzwarth, A.R. *FEBS Lett.* **2007**, *581*, 5435–5439.
(11) Tamiaki, H.; Shibata, R.; Mizoguchi, T. *Photochem. Photobiol.* **2007**, *83*, 152–162.
(12) Larsen, K.L.; Miller, M.; Cox, R.P. *Arch. Microbiol.* **1995**, *163*, 119–123.
(13) Steensgaard, D.B.; Cox, R.P.; Miller, M. *Photosynth. Res.* **1996**, *48*, 385–393.
(14) Tamiaki, H.; Miyata, S.; Kureishi, Y.; Tanikaga, R. *Tetrahedron* **1996**, *52*, 12421–12432.
(15) Miyatake, T.; Tamiaki, H.; Shinoda, H.; Fujiwara, M.; Matsushita, T. *Tetrahedron* **2002**, *58*, 9989–10000.
(16) Shibata, R.; Tamiaki, H. *Bioorg. Med. Chem.* **2006**, *14*, 2235–2241.
(17) Mizoguchi, T.; Tamiaki, H. *Bull. Chem. Soc. Jpn* **2007**, *80*, 2196–2202.
(18) Zupcanova, A.; Arellano, J.B.; Bina, D.; Kopecky, J.; Psencík, J.; Vacha, F. *Photochem. Photobiol.* **2008**, *84*, 1187–1194.
(19) Tamiaki, H.; Michitsuji, T.; Shibata, R. *Photochem. Photobiol. Sci.* **2008**, *7*, 1225–1230.
(20) Wahlund, T.M.; Woese, C.R.; Castenholz, R.W.; Madigan, M.T. *Arch. Microbiol.* **1991**, *156*, 81–90.
(21) Pierson, B.K.; Castenholz, R.W. *Arch. Microbiol.* **1974**, *100*, 5–24.
(22) Saga, Y.; Tamiaki, H. *J. Photochem. Photobiol. B* **2004**, *73*, 29–34.
(23) Saga, Y.; Miyatake, T.; Tamiaki, H. *Bioorg. Med. Chem. Lett.* **2002**, *12*, 1229–1231.
(24) Saga, Y.; Akai, S.; Miyatake, T.; Tamiaki, H. *Bioconjugate Chem.* **2006**, *17*, 988–994.